STRUCTURAL CHEMISTRY

ISSN 2053-2296

Triethanolaminate iron perchlorate revisited: change of space group, chemical composition and oxidation states in $[Fe_7(tea)_3(tea\text{-}H)_3](ClO_4)_2$ (tea-H_3 is triethanolamine)

Jitschaq A. van der Horn and Martin Lutz*

Bijvoet Center for Biomolecular Research, Crystal and Structural Chemistry, Faculty of Science, Utrecht University, Padualaan 8, 3584 CH Utrecht, The Netherlands. *Correspondence e-mail: m.lutz@uu.nl

Received 13 October 2017
Accepted 27 December 2017

Edited by I. D. Williams, Hong Kong University of Science and Technology, Hong Kong

Keywords: heptanuclear mixed-valence coordination cluster; pseudosymmetry; iron oxidation state; validation; crystal structure.

CCDC reference: 1813756

Supporting information: this article has supporting information at journals.iucr.org/c

The X-ray crystal structure of tris[*N*-(2-hydroxyethyl)-2,2′-iminodiethanolato]-tris(2,2′,2″-nitrilotriethanolato)tetrairon(II)triiron(III) bis(perchlorate), $[Fe_7(C_6H_{12}NO_3)_3(C_6H_{13}NO_3)_3](ClO_4)_2$ or $[Fe_7(tea)_3(tea\text{-}H)_3](ClO_4)_2$ (tea-H_3 is triethanolamine), is known from the literature [Liu *et al.* (2008). *Z. Anorg. Allg. Chem.* **634**, 778–783] as a heptanuclear coordination cluster. The space group was given as $I2_13$ and is reinvestigated in the present study. We find a new space-group symmetry of $Pa\bar{3}$ and could detect O—H hydrogens, which were missing in the original publication. Consequences on the Fe oxidation states are investigated with the bond-valence method, resulting in a mixed-valence core of four Fe^{II} and three Fe^{III} centres. Symmetry relationships between the two space groups and the average supergroup $Ia\bar{3}$ are discussed in detail.

1. Introduction

The crystal structure of triethanolaminate iron perchlorate is known from the literature in the noncentrosymmetric space group $I2_13$ with a unit-cell volume of 10849.9 (3) Å^3 (Liu *et al.*, 2008). The composition of the cation was given as $C_{36}H_{72}Fe_7N_6O_{18}$. There are three independent Fe centres. One Fe centre is on a threefold axis and two are on general positions. Based on bond lengths and charge balance, the original publication assigns an oxidation state +2 to Fe1 and +3 to both Fe2 and Fe3. The overall ratio between the +2 and +3 oxidation states is then 1:6. Bond-valence sum calculations were not conclusive and the authors could not exclude a mixed-valence situation. The Fe^{II} centre is octahedrally surrounded by six O atoms and the Fe^{III} centres are octahedrally surrounded by five O and one N atom. The Fe—O bond lengths are in the range 2.123 (6)–2.181 (5) Å for Fe^{II} and 1.953 (6)–2.183 (6) Å for Fe^{III}. In addition, there are two crystallographically independent perchlorate anions present on a threefold axis.

Validation with the *PLATON* software (Spek, 2009) clearly indicates the presence of a crystallographic inversion centre at $(\frac{1}{4}, \frac{1}{4}, \frac{1}{4})$. The program suggests a space-group change from $I2_13$ to $Ia\bar{3}$, giving a 100% fit. The maximum deviation for the non-H atoms in the cation is 0.09 Å. The validation software additionally warns of short intermolecular O···O distances. Atom O2 and symmetry-related O2^{iv} are separated by 2.574 (9) Å, and O5 and O5^{v} are separated by 2.649 (9) Å [symmetry codes: (iv) $-x, -y+\frac{1}{2}, z$; (v) $-x+\frac{1}{2}, y, -z+2$]. Such short intermolecular distances strongly suggest the presence of hydrogen bonds. Because of the symmetry relations, the missing O—H hydrogens must be located on or disordered

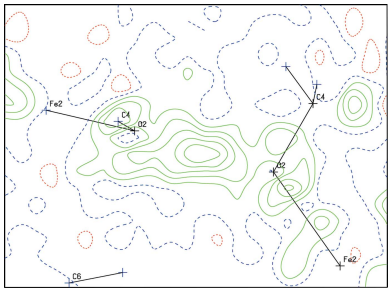

about special positions with occupancies of $\frac{1}{2}$. No H atoms at these positions are given in the original publication.

As the original reflection data were not available to us, we resynthesized the compound and performed a new X-ray diffraction experiment.

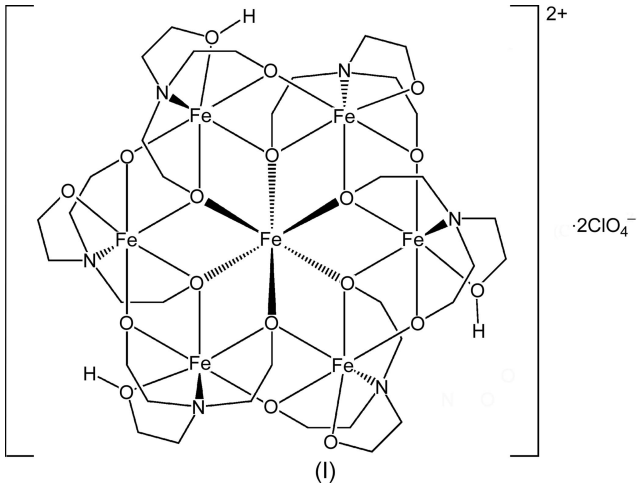

(I)

2. Experimental

2.1. Synthesis and crystallization

The synthesis of (I) was performed according to the literature procedure of Liu *et al.* (2008). $Fe(ClO_4)_2{\cdot}xH_2O$ (0.26 g; Aldrich) was dissolved in methanol (3 ml) in a test tube. Methanol (3 ml) was carefully layered on top. Afterwards, a solution of triethanolamine (0.53 ml) in methanol (10 ml) was added slowly on top. After 2 d, crystals suitable for X-ray diffraction had formed.

Table 1
Experimental details.

Crystal data	
Chemical formula	$[Fe_7(C_6H_{12}NO_3)_3(C_6H_{13}NO_3)_3]$-$(ClO_4)_2$
M_r	1469.87
Crystal system, space group	Cubic, $Pa\overline{3}$
Temperature (K)	100
a (Å)	22.0884 (6)
V (Å^3)	10776.9 (8)
Z	8
Radiation type	Mo $K\alpha$
μ (mm^{-1})	2.02
Crystal size (mm)	0.22 × 0.09 × 0.08
Data collection	
Diffractometer	Bruker Kappa APEXII
Absorption correction	Numerical (*SADABS*; Sheldrick, 2014)
T_{min}, T_{max}	0.687, 0.887
No. of measured, independent and observed [$I > 2\sigma(I)$] reflections	211368, 7962, 6121
R_{int}	0.055
(sin $\theta/\lambda)_{max}$ (Å^{-1})	0.808
Refinement	
$R[F^2 > 2\sigma(F^2)]$, $wR(F^2)$, S	0.028, 0.070, 1.02
No. of reflections	7962
No. of parameters	236
H-atom treatment	H atoms treated by a mixture of independent and constrained refinement
$\Delta\rho_{max}$, $\Delta\rho_{min}$ (e Å^{-3})	0.67, −0.47

Computer programs: *APEX3* (Bruker, 2016), *PEAKREF* (Schreurs, 2016), *EVAL15* (Schreurs *et al.*, 2010), *SADABS* (Sheldrick, 2014), *SHELXT* (Sheldrick, 2015*a*), *SHELXL2017* (Sheldrick, 2015*b*), *PLATON* (Spek, 2009) and *publCIF* (Westrip, 2010).

2.2. Refinement

Peak search and indexing on the strongest reflections confirmed the cubic *I*-centred cell of the literature (Liu *et al.*, 2008). Weak non-indexed reflections in the original frames and a two-dimensional reconstruction (simulated precession image) prompted us to integrate the data in the cubic *P*-cell of the same volume. Data collection was performed at 100 (2) K. Unit-cell determinations at 220 (2) and 293 (2) K show no phase transition. The weak superstructure reflections are still present at these temperatures.

Refinement in $I2_13$ used the coordinates of Liu *et al.* (2008) as the starting model. Transformation to the $Ia\overline{3}$ supergroup was performed with ADDSYM in *PLATON* (Spek, 2009). Structure solution in $Pa\overline{3}$ was performed with *SHELXT* (Sheldrick, 2015*a*).

A leverage analysis was performed with the program *HATTIE* (Parsons *et al.*, 2012). The design matrix for this purpose was created with the *CRYSTALS* software (Betteridge *et al.*, 2003).

In the final structure refinement in the space group $Pa\overline{3}$, all H atoms were located in difference Fourier maps. H atoms on C atoms were refined using a riding model, with C—H = 0.99 Å and U_{iso}(H) = 1.2U_{eq}(C). The O—H hydrogen was refined freely with an isotropic displacement parameter.

Crystal data, data collection and structure refinement details are summarized in Table 1.

3. Results and discussion

3.1. Structure determination in the space group $Ia\overline{3}$

Re-refinement of the literature structure with our newly collected reflection data in the space group $I2_13$ results in low R values of $R1$ [$I > 2\sigma(I)$] = 0.0252 and $wR2$ (all reflections) = 0.0633. The Flack (1983) parameter was included in the refinement as a two-component inversion twin and resulted in a value of x = 0.51 (5). A major problem in the refinement was the very large correlation matrix elements, with magnitudes up to 0.964, leading to an unstable refinement. Such unstable situations are known from the literature for structures where the inversion centre has accidentially been omitted (Marsh, 1995). As a consequence, we have to consider the Fe—O distances as unreliable in this space group.

As suggested by the *PLATON* software (see §1, *Introduction*), we transformed the $I2_13$ structure into the centrosymmetric supergroup $Ia\overline{3}$. As expected, this immediately solved the problem of large correlations. Here, there are no correlation matrix elements larger than 0.5. In the $Ia\overline{3}$ supergroup, there are only two independent Fe centres. Fe1 is on a special position with $\overline{3}$ symmetry (Wyckoff position *b*) and Fe2 is on a general position. The R values are now $R1$ [$I > 2\sigma(I)$] = 0.0239 and $wR2$ (all reflections) = 0.0606.

Table 2
Selected bond lengths (Å).

Fe1—O4	2.1353 (8)	Fe2—O1	2.2342 (8)
Fe1—O1	2.1719 (8)	Fe3—O3	1.9516 (8)
Fe2—O6^{i}	1.9814 (8)	Fe3—O5	1.9600 (8)
Fe2—O3	2.0198 (8)	Fe3—O6	1.9945 (8)
Fe2—N1	2.1873 (10)	Fe3—O1^{ii}	2.0270 (8)
Fe2—O4	2.1888 (8)	Fe3—O4	2.0989 (8)
Fe2—O2	2.2081 (9)	Fe3—N2	2.1774 (10)

Symmetry codes: (i) y, z, x; (ii) z, x, y.

Table 3
Hydrogen-bond geometry (Å, °).

D—H···A	D—H	H···A	D···A	D—H···A
O2—H2···O5^{iii}	0.89 (2)	1.73 (2)	2.6137 (13)	176 (2)

Symmetry code: (iii) $z, -x+\frac{1}{2}, y+\frac{1}{2}$.

In $Ia\bar{3}$, we have to be concerned about only one symmetry-independent short intermolecular O···O distance, namely the O2···O2^{vi} distance of 2.6144 (15) Å [symmetry code: (vi) $-x+1, -y+\frac{1}{2}, z$]. With the reflection data available, we are now able to investigate the residual density between these two atoms (Fig. 1). There is indeed a strong indication for the presence of an H atom close to the twofold axis, *viz.* the mid-point between O2 and O2^{vi}. This can be interpreted as a double-well situation (Gilli *et al.*, 2004). The H atom can only be half occupied, resulting in a molecular formula of $C_{36}H_{75}Fe_7N_6O_{18}$ for the cation. Of course, the larger number of H atoms will have consequences for the iron oxidation states. Fe—O distances of 2.1514 (8) Å for Fe1 and 1.9667 (8)–2.1655 (8) Å for Fe2 do not allow a clear distinction of oxidation state between the two independent iron centres. It should also be noted that the mean-square displacement amplitude along the Fe2—O2 bond is 0.0282 Å^2 and along the Fe2—O1^{vii} bond id 0.0185 Å^2, as calculated with *PLATON* (Spek, 2009) [symmetry code: (vii) $-y+\frac{1}{2}, -z+\frac{1}{2}, -x+\frac{1}{2}$].

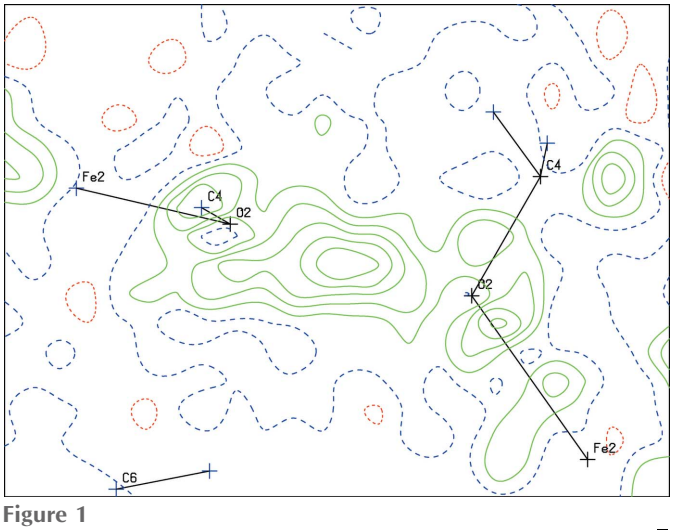

Figure 1
Residual density calculation around atom O2 in the space group $Ia\bar{3}$. Contour levels are drawn at −0.20 (red), 0.10 (blue) and 0.60 e Å^{-3} (green). Calculations were carried out with *PLATON* (Spek, 2009).

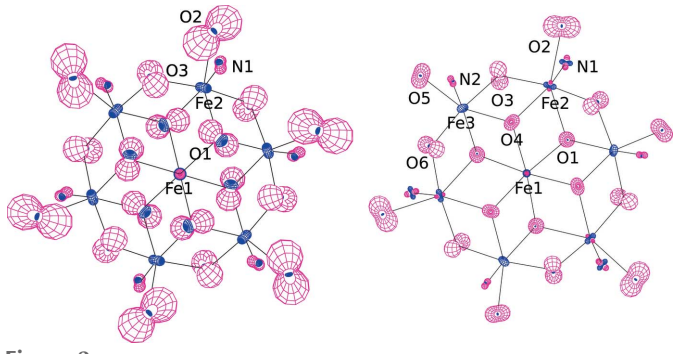

Figure 2
PEANUT plots (Hummel *et al.*, 1990) showing the difference between the measured displacement parameters and the parameters obtained by rigid-body analyses using the program *THMA11* (Schomaker & Trueblood, 1998). A scale factor of 6.15 was used for the r.m.s. surfaces. Red surfaces indicate positive differences and blue surfaces negative differences. Left: space group $Ia\bar{3}$; right: space group $Pa\bar{3}$.

These values are significantly larger than the limit of 0.001 Å^2 suggested by Hirshfeld (1976) for rigid bonds in organic molecules. Failure to this Hirshfeld rigid-bond test due to elongated displacement ellipsoids has been reported for the average structures of Jahn–Teller-distorted complexes [see, for example, Falvello (1997) and Smeets *et al.*, (2011)]. In the present structure, it can indicate an average structure as well. The physically unreasonable displacement behaviour can be seen clearly in a *PEANUT* plot (Fig. 2, left).

3.2. Structure determination in the space group $Pa\bar{3}$

A closer inspection of the diffraction pattern shows that reflections with $h+k+l = 2n$ are weak but not absent. Space

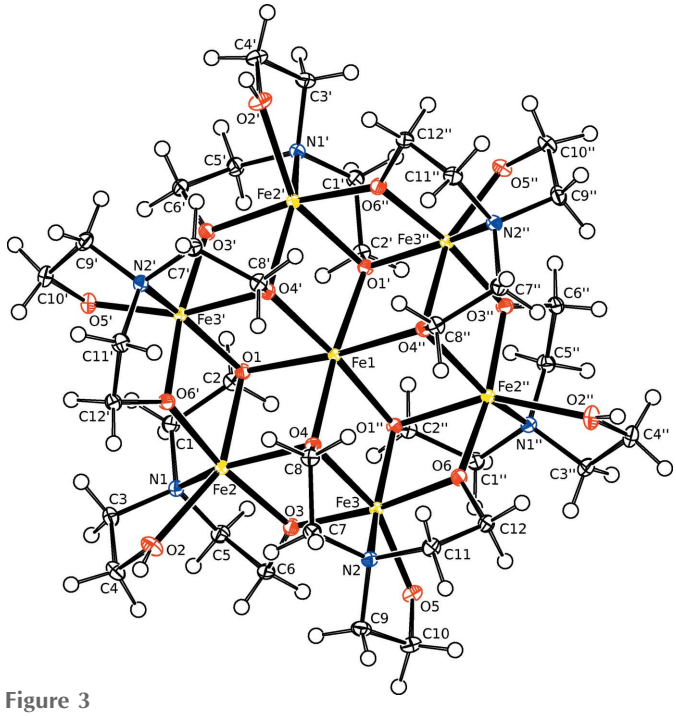

Figure 3
Displacement ellipsoid plot of the cation drawn at the 50% probability level. H atoms are drawn at arbitrary radii and perchlorate anions have been omitted for clarity. [Symmetry codes: (i) y, z, x; (ii) z, x, y.]

Table 4
Reflection statistics for the strong substructure and the weak superstructure reflections.

Agreement factors *R*1 and *wR*2 were calculated according to the *SHELXL* manual (Sheldrick, 2015*b*).

h+*k*+*l*	#	<*I*>	<σ>	<*I*>/<σ>	<*I*/σ>	*wR*2 (all reflections)	*R*1 [$I > 2\sigma(I)$]	# $I > 2\sigma(I)$
2*n*	3990	12721.86	495.31	25.68	46.01	0.0621	0.0233	84.29%
2*n*+1	3972	1654.41	131.84	12.55	15.64	0.0894	0.0412	69.44%
Total	7962	7198.77	313.97	22.93	30.85	0.0701	0.0282	76.88%

group $Ia\bar{3}$ thus represents an average structure and the true space group is subgroup $Pa\bar{3}$ with the same volume of the unit cell. After re-integration of the data based on the new cell, least-squares refinement in $Pa\bar{3}$ is stable. The largest element of the correlation matrix is here 0.521, just above the 0.5 cut-off. As in subgroup $I2_13$, Fe1 is on a threefold axis and Fe2 and Fe3 are on general positions (Fig. 3). The main difference is that subgroup $I2_13$ is obtained from $Ia\bar{3}$ by the removal of an inversion centre, while the true space group $Pa\bar{3}$ is obtained by the removal of translational symmetry. Consequences for the intramolecular geometry are minor but significant (Table 2, and see below). A major difference concerns the short intermolecular O···O contacts. In $I2_13$, this involves symmetry-related atom pairs O2/O2^{iv} and O5/O5^{viii} [symmetry codes: (iv) $-x, -y+\frac{1}{2}, z$; (viii) $-x+2, y, -z+2$], while in $Pa\bar{3}$, the two O atoms of the potential hydrogen bond are symmetry independent (Fig. 4). There is no symmetry element between the potential donor and acceptor O atoms.

Fig. 5 shows the residual electron density between atoms O2 and O5^{iii} [symmetry code: (iii) $z, -x+\frac{1}{2}, y+\frac{1}{2}$]. The H atom is clearly bound to O2 and can be introduced with full occupancy. Atom O5^{iii} is then the acceptor of the hydrogen bond (Table 3). From the nearly linear geometry and rather short O···O distance we conclude that the hydrogen bond is very strong. Overall, the hydrogen bonding leads to a three-dimensional network in the crystal. The different protonation state for atoms O2 and O5 is also reflected in the Fe—O distances. Fe2—O2 of 2.2081 (9) Å is significantly longer than Fe3—O5 with 1.9600 (8) Å. This difference can be used for the bond-valence calculations (see below). All Fe—O bonds now have reasonably low values for the Hirshfeld rigid-bond test, with a maximum of 0.0024 Å^2. Also, the *PEANUT* plot looks physically reasonable (Fig. 2, right). The *R* value of the rigid-body model improves from 0.238 ($Ia\bar{3}$) to 0.160 ($Pa\bar{3}$) ($R = \{\Sigma[(U_{obs} - U_{calc})^2]/\Sigma(U_{obs})^2\}^{1/2}$) (Schomaker & Trueblood, 1998).

The IR data given in the publication of Liu *et al.* (2008) show a broad peak at 3463 cm^{-1}. This can be an indication for the presence of an O—H group. We repeated the IR experiment on our crystals and indeed found a very broad peak in the same region.

The differences between the average structure in $Ia\bar{3}$ and the true structure in $Pa\bar{3}$ are mainly expressed in the weak superstructure reflections with $h+k+l = 2n + 1$. Reflection statistics are given in Table 4. The mean I/σ of the substructure reflections are 2.9-fold stronger than the superstructure reflections. Still, 69.44% of the superstructure reflections are stronger than the 2σ criterion. This pseudotranslation symmetry can also be seen in the Patterson map calculated

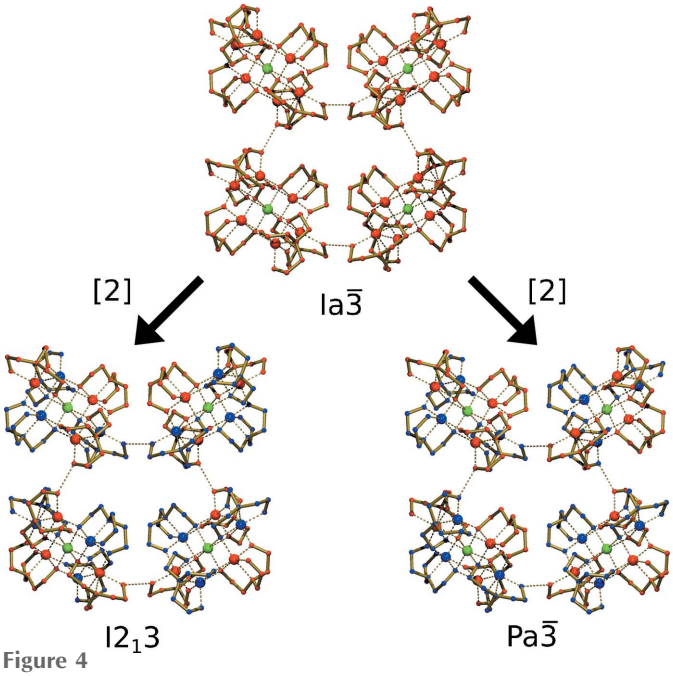

Figure 4
Coordination between adjacent cations in each of the described space groups. Dashed lines between the cations represent short (< 2.7 Å) O···O distances. Each colour represents a crystallographically independent part of the complex. The supergroup $Ia\bar{3}$ can be transformed into one of the subgroups $I2_13$ and $Pa\bar{3}$, both with subgroup index 2.

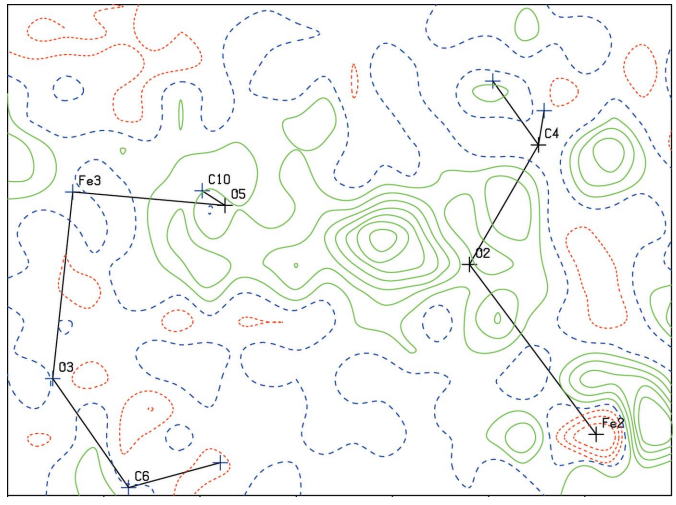

Figure 5
Residual density calculation around atom O2 in the space group $Pa\bar{3}$. The residual density peak is located 0.915 Å from O2. Contour levels are drawn at −0.40 (red), 0.10 (blue) and 0.70 (green) e Å^{-3}. Calculations were carried out with *PLATON* (Spek, 2009).

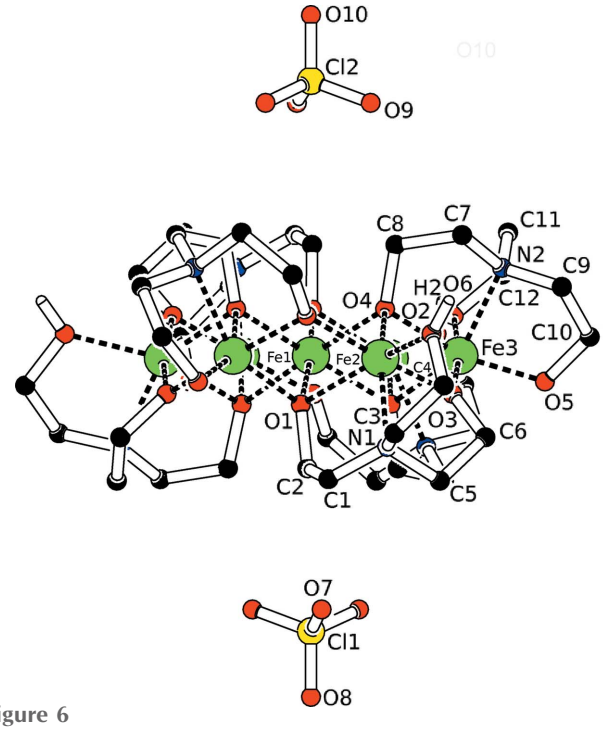

Figure 6
Side view of the title compound. The approximate inversion symmetry is mainly violated by the O—H hydrogen. C—H hydrogens have been omitted for clarity.

Table 5
Results of the leverage analysis performed with the program *HATTIE* (Parsons *et al.*, 2012).

The normalized value T^2 is a measure of the influence of a specific reflection on a refined parameter.

	h	*k*	*l*	T^2
x coordinate (H2)	3	1	5	10000
	3	3	3	7629.49
	3	5	7	7353.62
	5	1	7	7175.33
y coordinate (H2)	0	2	6	10000
	0	6	10	7304.21
	5	1	8	5936.25
	6	4	10	5243.41
z coordinate (H2)	5	0	6	10000
	4	6	7	5790.49
	1	0	8	5227.58
	3	4	6	4357.97

with *SHELXS97* (Sheldrick, 2008). The highest non-origin peak is at ($\frac{1}{2}$, $\frac{1}{2}$, $\frac{1}{2}$), with a height of 346 compared to the normalized height of 999 at the origin. Within the default tolerances, *PLATON* ADDSYM gives a 100% fit for *I*-centred superstructure $Ia\bar{3}$. The maximum deviation is 0.35 Å and involves the O2/O5 atom pair. The cation has an exact crystallographic C_3 symmetry and an approximate C_{3i} symmetry, with an r.m.s. deviation of 0.0750 Å for the non-H atoms (Pilati & Forni, 1998). The C_{3i} symmetry is mainly broken by the O—H hydrogens (Fig. 6).

A leverage analysis (Parsons *et al.*, 2012) gives a quantitative insight on the influence of certain observations on the refined parameters. We were especially interested in which reflections have the largest influence on the position of atom H2. The largest T^2 values for the *x*, *y* and *z* coordinates are given in Table 5. In the current setting of the coordinates, the most influencial reflections for the *x* and *z* coordinates all belong to the weak superstructure reflections with $h+k+l = 2n + 1$. The *y* coordinate does not have this dependency. Indeed, the O2$\cdots$O5^{iii} direction of the hydrogen bond is nearly perpendicular to the *b* axis, with an angle of 90.46 (4)°.

Table 6
Bond lengths (Å) from different refinements.

	Literature structure at room temperature (Liu *et al.*, 2008)	Present study at 100 K		
	$I2_13$	$I2_13$	$Ia\bar{3}$	$Pa\bar{3}$
Fe1—O	2.123 (6)–2.181 (5)	2.140 (4)–2.163 (5)	2.1514 (8)	2.1352 (8)–1.1719 (8)
Fe2—O	1.977 (6)–2.183 (6)	1.976 (4)–2.166 (5)	1.9667 (8)–2.1654 (8)	1.9814 (8)–2.2342 (8)
Fe3—O	1.953 (6)–2.151 (6)	1.956 (5)–2.165 (5)	–	1.9516 (8)–2.0989 (8)

Table 7
Bond-valence sums (BVS).

Entries for the literature structure were taken from the original publication. Entries for the present study were calculated using the *TopospPro* software (Version 5.3.0.3; Blatov *et al.*, 2014) with parameters from Brown (2016*b*): $R_0(Fe^{3+}—O)$ = 1.759 Å; $R_0(Fe^{2+}—O)$ = 1.734 Å; $R_0(Fe^{3+}—N)$ = 1.82 Å; $R_0(Fe^{2+}—N)$ = 1.76 Å. A *b* value of 0.37 was used for all bonds.

	Assumed state	Literature structure at room temperature (Liu *et al.*, 2008)	Present study at 100 K		
		$I2_13$	$I2_13$	$Ia\bar{3}$	$Pa\bar{3}$
Fe1	+2	1.82	1.94	1.94	1.93
	+3		2.08	2.08	2.07
Fe2	+2		2.40	2.40	2.11
	+3	2.53	2.60	2.61	2.30
Fe3	+2		2.40		2.75
	+3	2.73	2.61		2.97

3.3. Bond-valence analysis

As discussed above, the space group choice results in different symmetries of the Fe sites. A summary of the corresponding Fe—O distances is given in Table 6. We assume that the distances in $I2_13$ are unreliable because of an instable least-squares refinement. The distances in $Ia\bar{3}$ reflect the situation of an average structure. In the true space group $Pa\bar{3}$, there are three symmetry-independent Fe sites. The Fe—O distances for Fe3 (general position) are shorter than the distances for Fe1 (special position, threefold axis) and Fe2 (general position).

Based on the difference of bond lengths, Brown introduced the concept of bond-valence analysis for the determination of oxidation states (Brown, 2016*a*). An overview is shown in Table 7. The published values for the bond-valence sum (BVS) in the literature structure are rather inconclusive (Liu *et al.*, 2008). With the correct

space group choice $Pa\bar{3}$, we can conclude that atoms Fe1 and Fe2 are in a +2 oxidation state, while Fe3 is in a +3 oxidation state. This is consistent with the addition of O—H hydrogens, which were missing in the literature structure.

4. Conclusions

The current study was initiated because the *PLATON* validation software (Spek, 2009) hints on severe problems with the literature structure (Liu *et al.*, 2008). In the course of our investigations, it appeared that weak superstructure reflections were essential for the determination of the Fe oxidation states, as well as of the hydrogen-bonding situation. The situation is comparable to a recent study, where weak superstructure reflections were essential for the explanation of the hydrogen-bonded network of an organic molecule (Zarychta *et al.*, 2016).

The original publication of Liu *et al.* (2008) did not include reflection data. Even if they were available, it would be impossible to detect the missing translation symmetry and the original problem with reflection indexing. This can only be detected if the original diffraction images are available. Fortunately, there are now initiatives attempting to set up an archiving system for diffraction images (Kroon-Batenburg *et al.*, 2017; Helliwell *et al.*, 2017).

Acknowledgements

Fruitful discussions with the group Organic Chemistry and Catalysis (Utrecht University) are kindly acknowledged.

Funding information

Funding for this research was provided by: the Netherlands Organization for Scientific Research (NWO), which financed the purchase of the X-ray diffractometer.

References

Betteridge, P. W., Carruthers, J. R., Cooper, R. I., Prout, K. & Watkin, D. J. (2003). *J. Appl. Cryst.* **36**, 1487.
Blatov, V. A., Shevchenko, A. P. & Proserpio, D. M. (2014). *Cryst. Growth Des.* **14**, 3576–3586.
Brown, I. D. (2016*a*). In *The Chemical Bond in Inorganic Chemistry*. Oxford University Press.
Brown, I. D. (2016*b*). *Bond valence parameters*. http://www.iucr.org/_data/assets/file/0007/126574/bvparm2016.cif.
Bruker (2016). *APEX3*. Bruker AXS Inc., Madison, Wisconsin, USA.
Falvello, L. R. (1997). *J. Chem. Soc. Dalton Trans.* pp. 4463–4476.
Flack, H. D. (1983). *Acta Cryst.* A**39**, 876–881.
Gilli, P., Bertolasi, V., Pretto, L., Ferretti, V. & Gilli, G. (2004). *J. Am. Chem. Soc.* **126**, 3845–3855.
Helliwell, J. R., McMahon, B., Guss, J. M. & Kroon-Batenburg, L. M. J. (2017). *IUCrJ*, **4**, 714–722.
Hirshfeld, F. L. (1976). *Acta Cryst.* A**32**, 239–244.
Hummel, W., Hauser, J. & Bürgi, H.-B. (1990). *J. Mol. Graph.* **8**, 214–220.
Kroon-Batenburg, L. M. J., Helliwell, J. R., McMahon, B. & Terwilliger, T. C. (2017). *IUCrJ*, **4**, 87–99.
Liu, T., Wang, B.-W., Chen, Y.-H., Wang, Z.-M. & Gao, S. (2008). *Z. Anorg. Allg. Chem.* **634**, 778–783.
Marsh, R. E. (1995). *Acta Cryst.* B**51**, 897–907.
Parsons, S., Wagner, T., Presly, O., Wood, P. A. & Cooper, R. I. (2012). *J. Appl. Cryst.* **45**, 417–429.
Pilati, T. & Forni, A. (1998). *J. Appl. Cryst.* **31**, 503–504.
Schomaker, V. & Trueblood, K. N. (1998). *Acta Cryst.* B**54**, 507–514.
Schreurs, A. M. M. (2016). *PEAKREF*. University of Utrecht, The Netherlands.
Schreurs, A. M. M., Xian, X. & Kroon-Batenburg, L. M. J. (2010). *J. Appl. Cryst.* **43**, 70–82.
Sheldrick, G. M. (2008). *Acta Cryst.* A**64**, 112–122.
Sheldrick, G. M. (2014). *SADABS*. University of Göttingen, Germany.
Sheldrick, G. M. (2015*a*). *Acta Cryst.* A**71**, 3–8.
Sheldrick, G. M. (2015*b*). *Acta Cryst.* C**71**, 3–8.
Smeets, S., Parois, P., Bürgi, H.-B. & Lutz, M. (2011). *Acta Cryst.* B**67**, 53–62.
Spek, A. L. (2009). *Acta Cryst.* D**65**, 148–155.
Westrip, S. P. (2010). *J. Appl. Cryst.* **43**, 920–925.
Zarychta, B., Gianopoulos, C. G. & Pinkerton, A. A. (2016). *Bioorg. Med. Chem. Lett.* **26**, 1416–1418.

supporting information

Acta Cryst. (2018). C**74**, 125-130 [https://doi.org/10.1107/S2053229617018460]

Triethanolaminate iron perchlorate revisited: change of space group, chemical composition and oxidation states in $[Fe_7(tea)_3(tea\text{-}H)_3](ClO_4)_2$ (tea-H_3 is triethanolamine)

Jitschaq A. van der Horn and Martin Lutz

Computing details

Data collection: *APEX3* (Bruker, 2016); cell refinement: *PEAKREF* (Schreurs, 2016); data reduction: *EVAL15* (Schreurs *et al.*, 2010) and *SADABS* (Sheldrick, 2014); program(s) used to solve structure: SHELXT (Sheldrick, 2015a); program(s) used to refine structure: *SHELXL2017* (Sheldrick, 2015b); molecular graphics: *PLATON* (Spek, 2009); software used to prepare material for publication: *publCIF* (Westrip, 2010).

Tris[*N*-(2-hydroxyethyl)-2,2′-iminodiethanolato]tris(2,2′,2′′-\ nitrilotriethanolato)tetrairon(II)triiron(III) bis(perchlorate)

Crystal data

$[Fe_7(C_6H_{12}NO_3)_3(C_6H_{13}NO_3)_3](ClO_4)_2$
M_r = 1469.87
Cubic, $Pa\bar{3}$
a = 22.0884 (6) Å
V = 10776.9 (8) Å^3
Z = 8
$F(000)$ = 6056
D_x = 1.812 Mg m^{-3}
Mo $K\alpha$ radiation, λ = 0.71073 Å
Cell parameters from 104201 reflections
θ = 1.3–35.1°
μ = 2.02 mm^{-1}
T = 100 K
Block, black
0.22 × 0.09 × 0.08 mm

Data collection

Bruker Kappa APEXII diffractometer
Radiation source: sealed tube
φ and ω scans
Absorption correction: numerical (SADABS; Sheldrick, 2014)
T_{min} = 0.687, T_{max} = 0.887
211368 measured reflections
7962 independent reflections
6121 reflections with $I > 2\sigma(I)$
R_{int} = 0.055
θ_{max} = 35.1°, θ_{min} = 1.6°
h = −35→30
k = −34→35
l = −33→31

Refinement

Refinement on F^2
Least-squares matrix: full
$R[F^2 > 2\sigma(F^2)]$ = 0.028
$wR(F^2)$ = 0.070
S = 1.02
7962 reflections
236 parameters
0 restraints
Primary atom site location: dual
Secondary atom site location: difference Fourier map
Hydrogen site location: difference Fourier map
H atoms treated by a mixture of independent and constrained refinement
$w = 1/[\sigma^2(F_o^2) + (0.0318P)^2 + 4.712P]$ where $P = (F_o^2 + 2F_c^2)/3$

$(\Delta/\sigma)_{max}$ = 0.002
$\Delta\rho_{max}$ = 0.67 e Å^{-3}
$\Delta\rho_{min}$ = −0.47 e Å^{-3}

Special details

Geometry. All esds (except the esd in the dihedral angle between two l.s. planes) are estimated using the full covariance matrix. The cell esds are taken into account individually in the estimation of esds in distances, angles and torsion angles; correlations between esds in cell parameters are only used when they are defined by crystal symmetry. An approximate (isotropic) treatment of cell esds is used for estimating esds involving l.s. planes.

Fractional atomic coordinates and isotropic or equivalent isotropic displacement parameters (Å²)

	x	*y*	*z*	U_{iso}*/U_{eq}
Fe1	0.25330 (2)	0.25330 (2)	0.25330 (2)	0.00791 (5)
Fe2	0.22069 (2)	0.16731 (2)	0.36722 (2)	0.00893 (4)
Fe3	0.33830 (2)	0.13764 (2)	0.28373 (2)	0.00842 (4)
O1	0.17204 (4)	0.21290 (4)	0.29115 (4)	0.00986 (14)
O2	0.21869 (4)	0.12195 (4)	0.45628 (4)	0.01637 (17)
H2	0.2383 (9)	0.1233 (11)	0.4913 (9)	0.048 (7)*
O3	0.26809 (4)	0.10217 (4)	0.32397 (4)	0.01312 (16)
O4	0.29956 (4)	0.21244 (4)	0.32770 (4)	0.00978 (14)
O5	0.37899 (4)	0.05905 (4)	0.27734 (4)	0.01365 (16)
O6	0.40289 (4)	0.18411 (4)	0.24104 (4)	0.01275 (15)
N1	0.14858 (4)	0.10076 (4)	0.35394 (4)	0.01091 (17)
N2	0.40266 (4)	0.15008 (4)	0.35735 (4)	0.01108 (17)
C1	0.10275 (5)	0.13060 (5)	0.31484 (5)	0.0129 (2)
H1A	0.076640	0.156948	0.340002	0.015*
H1B	0.076764	0.099374	0.295911	0.015*
C2	0.13276 (5)	0.16854 (5)	0.26538 (5)	0.01151 (19)
H2A	0.156258	0.141764	0.238188	0.014*
H2B	0.101192	0.188918	0.240948	0.014*
C3	0.12445 (5)	0.08718 (6)	0.41514 (5)	0.0146 (2)
H3A	0.097115	0.051736	0.412797	0.017*
H3B	0.100542	0.122151	0.429773	0.017*
C4	0.17503 (6)	0.07400 (5)	0.45961 (5)	0.0152 (2)
H4A	0.158507	0.071214	0.501178	0.018*
H4B	0.194465	0.034891	0.449512	0.018*
C5	0.17540 (5)	0.04711 (5)	0.32310 (6)	0.0134 (2)
H5A	0.166443	0.049253	0.279232	0.016*
H5B	0.156514	0.009797	0.339230	0.016*
C6	0.24374 (5)	0.04385 (5)	0.33227 (5)	0.0126 (2)
H6A	0.252965	0.029135	0.373582	0.015*
H6B	0.261812	0.015364	0.302765	0.015*
C7	0.37356 (5)	0.18936 (5)	0.40332 (5)	0.0130 (2)
H7A	0.404749	0.207173	0.430125	0.016*
H7B	0.345497	0.165143	0.428525	0.016*
C8	0.33886 (5)	0.23950 (5)	0.37111 (5)	0.0121 (2)
H8A	0.314986	0.263136	0.400776	0.014*
H8B	0.367487	0.267273	0.350669	0.014*

C9	0.41247 (6)	0.08692 (5)	0.37804 (5)	0.0149 (2)
H9A	0.376760	0.072762	0.401131	0.018*
H9B	0.448238	0.085129	0.404990	0.018*
C10	0.42245 (5)	0.04634 (5)	0.32320 (6)	0.0146 (2)
H10A	0.463706	0.052964	0.306983	0.018*
H10B	0.419081	0.003389	0.335540	0.018*
C11	0.45825 (5)	0.17931 (6)	0.33281 (5)	0.0137 (2)
H11A	0.494455	0.160261	0.351123	0.016*
H11B	0.458364	0.222757	0.343807	0.016*
C12	0.46122 (5)	0.17298 (5)	0.26411 (5)	0.0130 (2)
H12A	0.490419	0.202435	0.247136	0.016*
H12B	0.474609	0.131682	0.252974	0.016*
Cl1	0.09580 (2)	0.09580 (2)	0.09580 (2)	0.01534 (9)
O7	0.08074 (5)	0.08564 (5)	0.15863 (5)	0.0266 (2)
O8	0.05841 (5)	0.05841 (5)	0.05841 (5)	0.0304 (4)
Cl2	0.41017 (2)	0.41017 (2)	0.41017 (2)	0.01490 (9)
O9	0.42281 (5)	0.34728 (5)	0.42264 (5)	0.0253 (2)
O10	0.44765 (5)	0.44765 (5)	0.44765 (5)	0.0281 (4)

Atomic displacement parameters (Å²)

	U^{11}	U^{22}	U^{33}	U^{12}	U^{13}	U^{23}
Fe1	0.00791 (5)	0.00791 (5)	0.00791 (5)	0.00099 (5)	0.00099 (5)	0.00099 (5)
Fe2	0.00892 (7)	0.00825 (7)	0.00963 (7)	0.00067 (5)	0.00126 (5)	0.00061 (5)
Fe3	0.00793 (7)	0.00863 (7)	0.00871 (7)	0.00104 (5)	0.00021 (5)	0.00058 (5)
O1	0.0105 (3)	0.0091 (3)	0.0101 (3)	−0.0005 (3)	0.0005 (3)	−0.0005 (3)
O2	0.0209 (4)	0.0160 (4)	0.0123 (4)	−0.0039 (3)	−0.0032 (3)	0.0034 (3)
O3	0.0131 (4)	0.0087 (3)	0.0176 (4)	0.0000 (3)	0.0047 (3)	0.0006 (3)
O4	0.0096 (3)	0.0099 (3)	0.0098 (3)	0.0005 (3)	−0.0010 (3)	0.0001 (3)
O5	0.0129 (4)	0.0120 (4)	0.0161 (4)	0.0025 (3)	−0.0014 (3)	−0.0013 (3)
O6	0.0079 (3)	0.0176 (4)	0.0127 (4)	0.0008 (3)	−0.0002 (3)	0.0042 (3)
N1	0.0105 (4)	0.0106 (4)	0.0117 (4)	0.0003 (3)	0.0015 (3)	0.0007 (3)
N2	0.0106 (4)	0.0115 (4)	0.0111 (4)	0.0018 (3)	−0.0005 (3)	0.0009 (3)
C1	0.0101 (5)	0.0132 (5)	0.0153 (5)	−0.0011 (4)	−0.0004 (4)	0.0016 (4)
C2	0.0114 (5)	0.0119 (5)	0.0112 (5)	−0.0016 (4)	−0.0015 (4)	−0.0007 (4)
C3	0.0138 (5)	0.0161 (5)	0.0138 (5)	−0.0016 (4)	0.0033 (4)	0.0027 (4)
C4	0.0204 (6)	0.0133 (5)	0.0118 (5)	−0.0028 (4)	0.0011 (4)	0.0025 (4)
C5	0.0141 (5)	0.0096 (5)	0.0164 (5)	−0.0009 (4)	0.0006 (4)	−0.0010 (4)
C6	0.0139 (5)	0.0079 (4)	0.0161 (5)	0.0002 (4)	0.0023 (4)	0.0011 (4)
C7	0.0138 (5)	0.0153 (5)	0.0101 (5)	0.0026 (4)	−0.0014 (4)	−0.0007 (4)
C8	0.0136 (5)	0.0111 (5)	0.0115 (5)	−0.0002 (4)	−0.0018 (4)	−0.0011 (4)
C9	0.0173 (5)	0.0136 (5)	0.0138 (5)	0.0030 (4)	−0.0017 (4)	0.0034 (4)
C10	0.0144 (5)	0.0111 (5)	0.0183 (5)	0.0030 (4)	−0.0020 (4)	0.0002 (4)
C11	0.0102 (5)	0.0159 (5)	0.0152 (5)	−0.0009 (4)	−0.0017 (4)	0.0004 (4)
C12	0.0083 (5)	0.0158 (5)	0.0148 (5)	0.0006 (4)	0.0005 (4)	0.0024 (4)
Cl1	0.01534 (9)	0.01534 (9)	0.01534 (9)	0.00135 (10)	0.00135 (10)	0.00135 (10)
O7	0.0310 (6)	0.0320 (6)	0.0166 (5)	0.0077 (4)	0.0056 (4)	0.0051 (4)
O8	0.0304 (4)	0.0304 (4)	0.0304 (4)	−0.0074 (4)	−0.0074 (4)	−0.0074 (4)

Cl2	0.01490 (9)	0.01490 (9)	0.01490 (9)	0.00088 (10)	0.00088 (10)	0.00088 (10)
O9	0.0321 (6)	0.0161 (4)	0.0278 (5)	0.0056 (4)	0.0044 (4)	0.0032 (4)
O10	0.0281 (4)	0.0281 (4)	0.0281 (4)	−0.0057 (4)	−0.0057 (4)	−0.0057 (4)

Geometric parameters (Å, º)

Fe1—O4^{i}	2.1352 (8)	C2—H2B	0.9900
Fe1—O4^{ii}	2.1352 (8)	C3—C4	1.5159 (17)
Fe1—O4	2.1353 (8)	C3—H3A	0.9900
Fe1—O1	2.1719 (8)	C3—H3B	0.9900
Fe1—O1^{i}	2.1719 (8)	C4—H4A	0.9900
Fe1—O1^{ii}	2.1719 (8)	C4—H4B	0.9900
Fe2—O6^{i}	1.9814 (8)	C5—C6	1.5247 (16)
Fe2—O3	2.0198 (8)	C5—H5A	0.9900
Fe2—N1	2.1873 (10)	C5—H5B	0.9900
Fe2—O4	2.1888 (8)	C6—H6A	0.9900
Fe2—O2	2.2081 (9)	C6—H6B	0.9900
Fe2—O1	2.2342 (8)	C7—C8	1.5233 (16)
Fe3—O3	1.9516 (8)	C7—H7A	0.9900
Fe3—O5	1.9600 (8)	C7—H7B	0.9900
Fe3—O6	1.9945 (8)	C8—H8A	0.9900
Fe3—O1^{ii}	2.0270 (8)	C8—H8B	0.9900
Fe3—O4	2.0989 (8)	C9—C10	1.5229 (17)
Fe3—N2	2.1774 (10)	C9—H9A	0.9900
O1—C2	1.4271 (13)	C9—H9B	0.9900
O2—C4	1.4345 (15)	C10—H10A	0.9900
O2—H2	0.89 (2)	C10—H10B	0.9900
O3—C6	1.4080 (13)	C11—C12	1.5252 (16)
O4—C8	1.4247 (14)	C11—H11A	0.9900
O5—C10	1.4235 (14)	C11—H11B	0.9900
O6—C12	1.4071 (14)	C12—H12A	0.9900
N1—C3	1.4836 (15)	C12—H12B	0.9900
N1—C1	1.4849 (15)	Cl1—O8	1.4302 (18)
N1—C5	1.4898 (15)	Cl1—O7^{i}	1.4448 (10)
N2—C7	1.4822 (15)	Cl1—O7^{ii}	1.4448 (10)
N2—C9	1.4839 (15)	Cl1—O7	1.4448 (10)
N2—C11	1.4896 (15)	Cl2—O10	1.4341 (19)
C1—C2	1.5282 (16)	Cl2—O9	1.4435 (10)
C1—H1A	0.9900	Cl2—O9^{i}	1.4435 (10)
C1—H1B	0.9900	Cl2—O9^{ii}	1.4435 (10)
C2—H2A	0.9900		

O4^{i}—Fe1—O4^{ii}	99.17 (3)	N1—C1—H1B	109.4
O4^{i}—Fe1—O4	99.16 (3)	C2—C1—H1B	109.4
O4^{ii}—Fe1—O4	99.16 (3)	H1A—C1—H1B	108.0
O4^{i}—Fe1—O1	77.45 (3)	O1—C2—C1	110.80 (9)
O4^{ii}—Fe1—O1	174.49 (3)	O1—C2—H2A	109.5
O4—Fe1—O1	85.73 (3)	C1—C2—H2A	109.5

O4^{i}—Fe1—O1^{i}	85.73 (3)	O1—C2—H2B	109.5
O4^{ii}—Fe1—O1^{i}	77.44 (3)	C1—C2—H2B	109.5
O4—Fe1—O1^{i}	174.49 (3)	H2A—C2—H2B	108.1
O1—Fe1—O1^{i}	97.86 (3)	N1—C3—C4	111.37 (10)
O4^{i}—Fe1—O1^{ii}	174.49 (3)	N1—C3—H3A	109.4
O4^{ii}—Fe1—O1^{ii}	85.73 (3)	C4—C3—H3A	109.4
O4—Fe1—O1^{ii}	77.45 (3)	N1—C3—H3B	109.4
O1—Fe1—O1^{ii}	97.86 (3)	C4—C3—H3B	109.4
O1^{i}—Fe1—O1^{ii}	97.86 (3)	H3A—C3—H3B	108.0
O6^{i}—Fe2—O3	170.08 (4)	O2—C4—C3	108.69 (9)
O6^{i}—Fe2—N1	107.99 (4)	O2—C4—H4A	110.0
O3—Fe2—N1	80.52 (4)	C3—C4—H4A	110.0
O6^{i}—Fe2—O4	96.25 (3)	O2—C4—H4B	110.0
O3—Fe2—O4	73.93 (3)	C3—C4—H4B	110.0
N1—Fe2—O4	146.33 (3)	H4A—C4—H4B	108.3
O6^{i}—Fe2—O2	90.60 (3)	N1—C5—C6	111.74 (9)
O3—Fe2—O2	96.23 (4)	N1—C5—H5A	109.3
N1—Fe2—O2	78.46 (4)	C6—C5—H5A	109.3
O4—Fe2—O2	125.30 (3)	N1—C5—H5B	109.3
O6^{i}—Fe2—O1	74.48 (3)	C6—C5—H5B	109.3
O3—Fe2—O1	102.40 (3)	H5A—C5—H5B	107.9
N1—Fe2—O1	81.48 (3)	O3—C6—C5	108.54 (9)
O4—Fe2—O1	82.97 (3)	O3—C6—H6A	110.0
O2—Fe2—O1	149.87 (3)	C5—C6—H6A	110.0
O3—Fe3—O5	92.38 (4)	O3—C6—H6B	110.0
O3—Fe3—O6	172.02 (4)	C5—C6—H6B	110.0
O5—Fe3—O6	95.38 (4)	H6A—C6—H6B	108.4
O3—Fe3—O1^{ii}	95.38 (3)	N2—C7—C8	108.89 (9)
O5—Fe3—O1^{ii}	120.80 (3)	N2—C7—H7A	109.9
O6—Fe3—O1^{ii}	79.04 (3)	C8—C7—H7A	109.9
O3—Fe3—O4	77.37 (3)	N2—C7—H7B	109.9
O5—Fe3—O4	156.56 (3)	C8—C7—H7B	109.9
O6—Fe3—O4	96.05 (3)	H7A—C7—H7B	108.3
O1^{ii}—Fe3—O4	81.53 (3)	O4—C8—C7	108.41 (9)
O3—Fe3—N2	103.25 (4)	O4—C8—H8A	110.0
O5—Fe3—N2	82.31 (4)	C7—C8—H8A	110.0
O6—Fe3—N2	79.70 (4)	O4—C8—H8B	110.0
O1^{ii}—Fe3—N2	149.83 (4)	C7—C8—H8B	110.0
O4—Fe3—N2	79.70 (3)	H8A—C8—H8B	108.4
C2—O1—Fe3^{i}	120.46 (7)	N2—C9—C10	109.24 (9)
C2—O1—Fe1	129.12 (7)	N2—C9—H9A	109.8
Fe3^{i}—O1—Fe1	100.98 (3)	C10—C9—H9A	109.8
C2—O1—Fe2	106.43 (6)	N2—C9—H9B	109.8
Fe3^{i}—O1—Fe2	98.15 (3)	C10—C9—H9B	109.8
Fe1—O1—Fe2	94.43 (3)	H9A—C9—H9B	108.3
C4—O2—Fe2	113.21 (7)	O5—C10—C9	110.63 (9)
C4—O2—H2	108.0 (15)	O5—C10—H10A	109.5
Fe2—O2—H2	138.7 (14)	C9—C10—H10A	109.5

C6—O3—Fe3	136.90 (7)	O5—C10—H10B	109.5
C6—O3—Fe2	113.09 (7)	C9—C10—H10B	109.5
Fe3—O3—Fe2	109.96 (4)	H10A—C10—H10B	108.1
C8—O4—Fe3	113.16 (6)	N2—C11—C12	110.96 (9)
C8—O4—Fe1	129.21 (7)	N2—C11—H11A	109.4
Fe3—O4—Fe1	99.88 (3)	C12—C11—H11A	109.4
C8—O4—Fe2	114.05 (7)	N2—C11—H11B	109.4
Fe3—O4—Fe2	98.66 (3)	C12—C11—H11B	109.4
Fe1—O4—Fe2	96.80 (3)	H11A—C11—H11B	108.0
C10—O5—Fe3	115.63 (7)	O6—C12—C11	107.76 (9)
C12—O6—Fe2^{ii}	137.14 (7)	O6—C12—H12A	110.2
C12—O6—Fe3	113.19 (7)	C11—C12—H12A	110.2
Fe2^{ii}—O6—Fe3	108.30 (4)	O6—C12—H12B	110.2
C3—N1—C1	112.01 (9)	C11—C12—H12B	110.2
C3—N1—C5	113.50 (9)	H12A—C12—H12B	108.5
C1—N1—C5	110.99 (9)	O8—Cl1—O7^{i}	109.39 (5)
C3—N1—Fe2	105.98 (7)	O8—Cl1—O7^{ii}	109.39 (5)
C1—N1—Fe2	106.02 (7)	O7^{i}—Cl1—O7^{ii}	109.55 (5)
C5—N1—Fe2	107.84 (7)	O8—Cl1—O7	109.40 (5)
C7—N2—C9	113.75 (9)	O7^{i}—Cl1—O7	109.55 (5)
C7—N2—C11	110.68 (9)	O7^{ii}—Cl1—O7	109.55 (5)
C9—N2—C11	113.53 (9)	O10—Cl2—O9	109.50 (5)
C7—N2—Fe3	107.60 (7)	O10—Cl2—O9^{i}	109.50 (5)
C9—N2—Fe3	101.93 (7)	O9—Cl2—O9^{i}	109.45 (5)
C11—N2—Fe3	108.73 (7)	O10—Cl2—O9^{ii}	109.50 (5)
N1—C1—C2	111.32 (9)	O9—Cl2—O9^{ii}	109.44 (5)
N1—C1—H1A	109.4	O9^{i}—Cl2—O9^{ii}	109.45 (5)
C2—C1—H1A	109.4		

C3—N1—C1—C2	154.85 (10)	C9—N2—C7—C8	−152.83 (10)
C5—N1—C1—C2	−77.15 (12)	C11—N2—C7—C8	77.95 (11)
Fe2—N1—C1—C2	39.70 (10)	Fe3—N2—C7—C8	−40.72 (10)
Fe3^{i}—O1—C2—C1	−69.16 (10)	Fe3—O4—C8—C7	−38.20 (10)
Fe1—O1—C2—C1	151.10 (7)	Fe1—O4—C8—C7	−164.36 (7)
Fe2—O1—C2—C1	41.01 (10)	Fe2—O4—C8—C7	73.53 (9)
N1—C1—C2—O1	−57.29 (12)	N2—C7—C8—O4	52.65 (12)
C1—N1—C3—C4	−163.54 (10)	C7—N2—C9—C10	161.48 (10)
C5—N1—C3—C4	69.81 (12)	C11—N2—C9—C10	−70.76 (12)
Fe2—N1—C3—C4	−48.36 (11)	Fe3—N2—C9—C10	45.98 (10)
Fe2—O2—C4—C3	−26.94 (12)	Fe3—O5—C10—C9	19.09 (12)
N1—C3—C4—O2	51.07 (13)	N2—C9—C10—O5	−45.53 (13)
C3—N1—C5—C6	−95.22 (11)	C7—N2—C11—C12	−135.90 (10)
C1—N1—C5—C6	137.60 (10)	C9—N2—C11—C12	94.76 (11)
Fe2—N1—C5—C6	21.87 (11)	Fe3—N2—C11—C12	−17.93 (11)
Fe3—O3—C6—C5	−137.18 (9)	Fe2^{ii}—O6—C12—C11	146.42 (9)

Fe2—O3—C6—C5	45.75 (11)	Fe3—O6—C12—C11	−49.03 (11)
N1—C5—C6—O3	−43.95 (13)	N2—C11—C12—O6	42.43 (13)

Symmetry codes: (i) *y*, *z*, *x*; (ii) *z*, *x*, *y*.

Hydrogen-bond geometry (Å, º)

D—H···*A*	*D*—H	H···*A*	*D*···*A*	*D*—H···*A*
O2—H2···O5^{iii}	0.89 (2)	1.73 (2)	2.6137 (13)	176 (2)

Symmetry code: (iii) *z*, −*x*+1/2, *y*+1/2.